LIMNOLOGY
and
OCEANOGRAPHY

ASLO

Limnol. Oceanogr. 65, 2020, 1136–1148

doi: 10.1002/lno.11376

Nutrient regulation of late spring phytoplankton blooms in the midlatitude North Atlantic

Thomas J. Browning,[1*] **Ali A. Al-Hashem**,[1] **Mark J. Hopwood**,[1] **Anja Engel**,[1] **Ewan D. Wakefield**,[2] **Eric P. Achterberg**[1]

[1]Marine Biogeochemistry Division, GEOMAR Helmholtz Centre for Ocean Research Kiel, Kiel, Germany
[2]Institute of Biodiversity, Animal Health and Comparative Medicine, University of Glasgow, Glasgow, UK

Abstract

The duration and magnitude of the North Atlantic spring bloom impacts both higher trophic levels and oceanic carbon sequestration. Nutrient exhaustion offers a general explanation for bloom termination, but detail on which nutrients and their relative influence on phytoplankton productivity, community structure, and physiology is lacking. Here, we address this using nutrient addition bioassay experiments conducted across the midlatitude North Atlantic in June 2017 (late spring). In four out of six experiments, phytoplankton accumulated over 48–72 h following individual additions of either iron (Fe) or nitrogen (N). In the remaining two experiments, Fe and N were serially limiting, that is, their combined addition sequentially enhanced phytoplankton accumulation. Silicic acid (Si) added in combination with N + Fe led to further chlorophyll *a* (Chl *a*) enhancement at two sites. Conversely, addition of zinc, manganese, cobalt, vitamin B_{12}, or phosphate in combination with N + Fe did not. At two sites, the simultaneous supply of all six nutrients, in combination with N + Fe, also led to no further Chl *a* enhancement, but did result in an additional 30–60% particulate carbon accumulation. This particulate carbon accumulation was not matched by a Redfield equivalent of particulate N, characteristic of high C:N organic exudates that enhance cell aggregation and sinking. Our results suggest that growth rates of larger phytoplankton were primarily limited by Fe and/or N, making the availability of these nutrients the main bottom-up factors contributing to spring bloom termination. In addition, the simultaneous availability of other nutrients could modify bloom characteristics and carbon export efficiency.

The mid-to-high latitude North Atlantic is characterized by a springtime peak in phytoplankton concentrations and sinking of organic matter, which transfers around 0.5–2 GtC yr^{-1} to the ocean interior (Sanders et al. 2014). Key mechanisms underlying this ecological event have been identified: in winter, phytoplankton growth is light-limited, while deep surface mixed layers act to reduce losses to grazing (Behrenfeld and Boss 2018); In spring, stratification, higher solar angles, and longer daylength allow for greater light availability for photosynthesis, enhancing growth rates (Sverdrup 1953; Mahadevan et al. 2012; Mignot et al. 2018). Together this leads to surface phytoplankton accumulation (Behrenfeld and Boss 2018). Surface macronutrient removal scales with carbon drawdown and peaks over several weeks in spring (Buesseler et al. 1992; Körtzinger et al. 2008). As in many other oceanographic regions (Agustí et al. 2015), sinking phytoplankton—which mediate the surface to deep ocean carbon flux—are dominated by bloom-forming diatoms (Billett et al. 1983; Lampitt 1985; Smetacek 1985, 1999; Alldredge and Gotschalk 1989; Turner 2002; Buesseler and Boyd 2009; Martin et al. 2011; Rynearson et al. 2013).

Despite dominating sinking fluxes, many observational studies of the North Atlantic spring bloom have found diatom blooming to be spatially constrained, short-lived, or absent (Williams and Claustre 1991; Barlow et al. 1993; Lochte et al. 1993; Sieracki et al. 1993; Verity et al. 1993; Allen et al. 2005; Moore et al. 2005; Leblanc et al. 2009; Martin et al. 2011; Rynearson et al. 2013; Daniels et al. 2015). Instead, assemblages dominated by smaller nanophytoplankton (2–20 μm), which sink more slowly and are strongly grazer-constrained, are more common (Barlow et al. 1993; Leblanc et al. 2009; Daniels et al. 2015). Combined with observations of transient, high diatom export events at depth (Billett et al. 1983; Martin et al. 2011), this suggests strong constraint(s) on the growth and sinking of large, bloom-forming diatoms (Smetacek 1985,

*Correspondence: tbrowning@geomar.de

Additional Supporting Information may be found in the online version of this article.

1999; Buesseler and Boyd 2009; Martin et al. 2011; Rynearson et al. 2013; Agustí et al. 2015).

Multiple studies have invoked nutrient availability to explain the regulation of open ocean North Atlantic diatom blooms following relief of light limitation in early spring. However, there is a lack of consensus on which combinations of nutrients are limiting. In the high latitude Irminger Basin, community-level Fe stress has been found in summer—demonstrated by enhanced apparent photochemical efficiencies of photosystem II (PSII) (F_v/F_m) and chlorophyll *a* (Chl *a*) biomass following Fe supply (Nielsdóttir et al. 2009; Ryan-Keogh et al. 2013). Phytoplankton growth following Fe supply has also been found to deplete N to secondary limiting levels, that is, where Fe + N supply leads to enhanced phytoplankton accumulation over supply of Fe only (Ryan-Keogh et al. 2013). In addition, low concentrations of Si have been implicated as limiting to diatoms, and zinc (Zn), cobalt (Co), and vitamin B_{12} depletion have been suggested as potentially having coregulatory roles (Lochte et al. 1993; Sieracki et al. 1993; Ellwood and van den Berg 2000, 2001; Allen et al. 2005; Henson et al. 2006; Panzeca et al. 2008; Leblanc et al. 2009; Martin et al. 2011). Supporting the potential for multiple resource controls, recent GEOTRACES surveys suggest that multiple macro and micronutrients could be simultaneously approaching springtime codeficiency in North Atlantic seawater (Moore 2016). In summary, while transient blooms of diatoms might be critical for carbon and nutrient budgets in the North Atlantic, evidence is lacking to support specific constraints on their growth.

In order to constrain potential nutrient controls on phytoplankton blooms experimentally, we conducted bioassays during a cruise traversing the midlatitude North Atlantic (43–53°N) in late spring. Based on calculations of resource deficiency using available (micro-)nutrient data (Moore 2016), alongside prior experimental observations (Blain et al. 2004; Moore et al. 2006; Nielsdóttir et al. 2009; Ryan-Keogh et al. 2013), we predicted a priori that either Fe or N would be either primary limiting, colimiting, or serially limiting to both overall system productivity and diatom growth throughout the study region. As such, we tested for primary, secondary, or colimitation by these two nutrients by supplying these nutrients alone and in combination. Then, in parallel treatments with N + Fe limitation fully relived, we tested for co-/tertiary limitation of bloom formation by supplying six extra nutrients potentially depleted to limiting levels: Phosphorus (P), Si, Co, manganese (Mn), Zn, and vitamin B_{12}. Finally, we tested for co-/serial limitation by more than three nutrients at the same time by supplying all nutrients in combination.

Methods

General

Fieldwork was conducted on the *RRS Discovery* in June 2017 (DY080), along a cruise track between Southampton (UK) and St Johns (Canada) (Fig. 1). Seawater was pumped from ~ 2 m depth into a trace-metal-clean laboratory (over-pressurized with high efficiency particulate air (HEPA)-filtered air) from a towed water sampling device (towed fish) via acid-washed tubing and a Teflon bellows pump (Dellmeco) powered by filtered compressed air. Conductivity-Temperature-Depth casts to 500 m depth were performed throughout the cruise track. Mixed layer depths were calculated as the depth of 0.03 kg m^{-3} density changes relative to a 10 m reference density value (Montegut et al., 2004). Daily satellite-derived Chl *a* fields (4 km resolution, L3 standard mapped images) from the Visible and Infrared Imager/Radiometer Suite (VIIRS) instrument (Ocean Color Index, OCI, algorithm) were downloaded from the NASA Ocean Color website for the period April–July 2017.

Bioassay experiments

Experiments followed previously published protocols (Browning et al. 2017). Unscreened seawater, pumped from the trace-metal-clean sampling device, was used to fill a 60-liter carboy, agitated to homogenize, and dispensed in random order into 2-liter (control, N + Fe) or 1-liter (all remaining treatments) acid-washed polycarbonate bottles (Nalgene). Before and/or after filling the 60-liter carboy, samples were collected for dissolved macronutrient and trace element analysis (see below). Approximately 8-liter from the 60-liter carboy was collected at the beginning and end of the incubation bottle filling procedure in order to measure initial phytoplankton concentrations, community structure, and photophysiology (see below). Incubation bottles were spiked in triplicate with nutrient combinations to the following amended concentrations: N: 1 μmol L^{-1} $NaNO_3$ + 1 μmol L^{-1} NH_4Cl; P: 0.2 μmol L^{-1} NaH_2PO_4; Si: 1 μmol L^{-1} Na_2O_3Si; Fe: 2 nmol L^{-1} $FeCl_3$, Mn: 2 nmol L^{-1} $MnCl_2$; Zn: 2 nmol L^{-1} $ZnCl_2$, Co: 2 nmol L^{-1} $CoCl_2$; vitamin B_{12}: 100 pmol L^{-1}. Macronutrient and B_{12} nutrient stocks were previously passed through a prepared column of cation exchange resin to remove trace element contamination (Chelex, BioRad). Fe, Co, Mn, and Zn were prepared from 99+% purity salts, stabilized in 0.01 mol L^{-1} HCl (Fisher Optima grade HCl diluted in Milli-Q water). Bottles were capped, sealed with Parafilm, bagged, and placed in an on-deck incubator for 48–72 h. The incubator was screened with blue filters (Lee Filters "Blue Lagoon"), to provide an irradiance around 35% of above surface values, and was subjected to continuous seawater exchange from the ship's underway flow-through supply. Following the incubation period, bottles were removed and 500 mL of each triplicate replicate was subsampled for collection/analysis of Chl *a*, Fast Repetition Rate fluorometry, and flow cytometry. The remaining 500 mL from each triplicate treatment was pooled for collection of samples for high-performance liquid chromatography (HPLC)-derived pigments (0.6–1 L), particulate organic carbon/nitrogen (POC/PON) (0.2–0.5 L), biogenic silicate (BSi) (0.14–0.6 L), and microscopy (60 mL). For the control and N + Fe treatments only, samples for macronutrients

were also filtered through precleaned (0.1 mol L^{-1} Fisher Optima grade HCl soak for 48 h followed by deionized water rinse) 0.2 μm Sterivex filter units (Millipore) under a laminar flow hood.

Macronutrients and trace elements

Dissolved trace element samples were collected in 125 mL low-density polyethylene bottles following direct in-line filtration (0.45 + 0.2 μm Sartorius Sartobran 300 filter units) from the Teflon pump-powered seawater supply. Samples were acidified within 24 h with 140 μL concentrated HCl (Optima Grade, Fisher). Samples were preconcentrated on a Sea*FAST* device and analyzed for Fe concentrations using an Element XR ICP-MS (directly following the method of Rapp et al. 2017). The detection limit for Fe using this method is 28.8 pmol L^{-1} (Rapp et al. 2017). Macronutrient samples (nitrite plus nitrate; hereafter referred to as simply as nitrate, phosphate, and silicic acid) were collected 0.2 μm filtered, as for trace element samples, into acid-washed 50 mL polypropylene tubes and frozen directly at −20°C. Concentrations were determined upon return to a land-based laboratory following thawing for 24 h at 5°C and analysis using a nutrient autoanalyzer system (QuAAtro, SEAL Analytical). Detection limits for the macronutrient analyses, calculated as three times the standard deviation of a blank measured during the analytical run, were: nitrate + nitrite = 0.08 μmol L^{-1}; phosphate = 0.03 μmol L^{-1}; and silicic acid = 0.09 μmol L^{-1}.

Phytoplankton biomass and community structure

Samples for Chl *a* were filtered (100 mL) onto 25 mm diameter glass microfibre filter (GFF) filters, extracted in the dark for approximately 24 h in 10 mL 90% (by volume) acetone at −20°C, and analyzed on a precalibrated Turner Designs Trilogy laboratory fluorometer (Welschmeyer 1994). Samples for flow cytometry analysis were fixed with 1% paraformaldehyde (final concentration), mixed with a vortex, left for 10 min at room temperature in the dark, and then placed directly into a −80°C freezer. Samples were analyzed on return to shore using a FACSCalibur flow cytometer (Becton Dickenson, Oxford, United Kingdom). Cell counts were determined using CellQuest software (Becton Dickenson) following procedures described in Davey et al. (2008). Identification of divisions between pico- and nanophytoplankton was aided by analysis of 2 μm filtrates for control and N + Fe samples in each experiment (N + Fe samples typically showing enhanced fluorescence per cell).

Samples for HPLC were filtered through 25 mm diameter GFF filters and placed directly into a −80°C freezer. Following the ship's return to port, samples were transported to the laboratory on dry ice but thawed during transport. The duration in the thawed state before refreezing to −80°C was between 0 and 12 h. Samples were, nevertheless, analyzed following the method of Van Heukelem and Thomas (2001). Samples were extracted in 90% acetone in plastic vials using glass beads in a cell mill, centrifuged (10 min, 5200 rpm, 4°C), and then the supernatant was filtered through 0.2 μm polytetrafluoroethylene (PTFE) filters (VWR International) and analyzed by reverse-phase HPLC (Dionex UltiMate 3000 LC system, Thermo Scientific). Pigment standards were acquired from Sigma-Aldrich (USA) and the International Agency for 14C Determination (Denmark). Recovery of total Chl *a* (Chl *a* + divinyl Chl *a*) from the HPLC analysis was approximately 20% in comparison to parallel, fluorometrically determined concentrations performed on ship. However, within the HPLC pigment data set itself, Chl *a* correlated near-linearly with summed diagnostic pigments (DP) (Chl $a = 1.1 \times DP - 0.01$; $R^2 = 0.78$; $p < 1 \times 10^{-15}$; $n = 195$), suggesting, despite notable pigment degradation, a relatively internally consistent data set (Trees et al. 2000). Regardless, all HPLC pigment data were interpreted only qualitatively via approximation of phytoplankton size groups (Uitz et al. 2006).

Samples from select nutrient treatments were preserved for microscopy analysis (60 mL; amber HDPE Nalgene bottles) using 0.2 mL alkaline Lugol's solution. Cells from 10–50 mL samples were concentrated in settling chambers for 24 h, then viewed and photographed using an inverted microscope (Zeiss Axiovert) at ×100 and ×200 magnification.

POC/PON and BSi

Samples for POC/N were filtered through combusted (6 h at 450°C) 25 mm diameter GFF filters. Filters were then oven-dried on ship at 50°C for 24 h. Filters were subject to sulfurous acid fuming to remove the contribution of particulate inorganic carbon, re-dried at 50°C for 24 h and then pelleted in tin boats (Elementar). Analyses were conducted using an elemental analyzer (Euro Elemental Analyser), using a set of known masses of acetanilide as standards. The contribution of particulate inorganic nitrogen to total particulate nitrogen measured was assumed to be negligible. Samples for BSi were filtered through 25 mm diameter 0.8 μm pore size polycarbonate filters (Whatman Nuclepore) and oven-dried on ship at 50°C for 24 h. Samples were digested in 4 mL 0.2 mol L^{-1} NaOH (Sigma-Aldrich) at 90°C for 2 h in acid-washed 15 mL polypropelene tubes (Rotilabo, Carl Roth). Following cooling, samples were neutralized with 10 mL 0.1 mol L^{-1} HCl (Fisher Optima grade, diluted in deionized water) and analyzed for dissolved silicic acid on a SEAL QuAAtro nutrient autoanalyzer system (SEAL Analytical). Digested blank filters yielded silicic acid concentrations below the detection limit (< 0.1 μmol L^{-1}).

Phytoplankton photophysiology

A FASTOcean Fast Repetition Rate fluorometer (Chelsea Technologies Group) was used to characterize community-level phytoplankton photophysiology. A protocol of 100 × 1 μs blue flashes with 1 μs dark intervals (excitation phase) followed by 25 × 1 μs flashes with 84 μs dark intervals (relaxation phase) was used. Fluorescence transients were fit automatically in FASTPro8 software using the model of Kolber et al. (1998) to yield values of minimum fluorescence (F_o) and

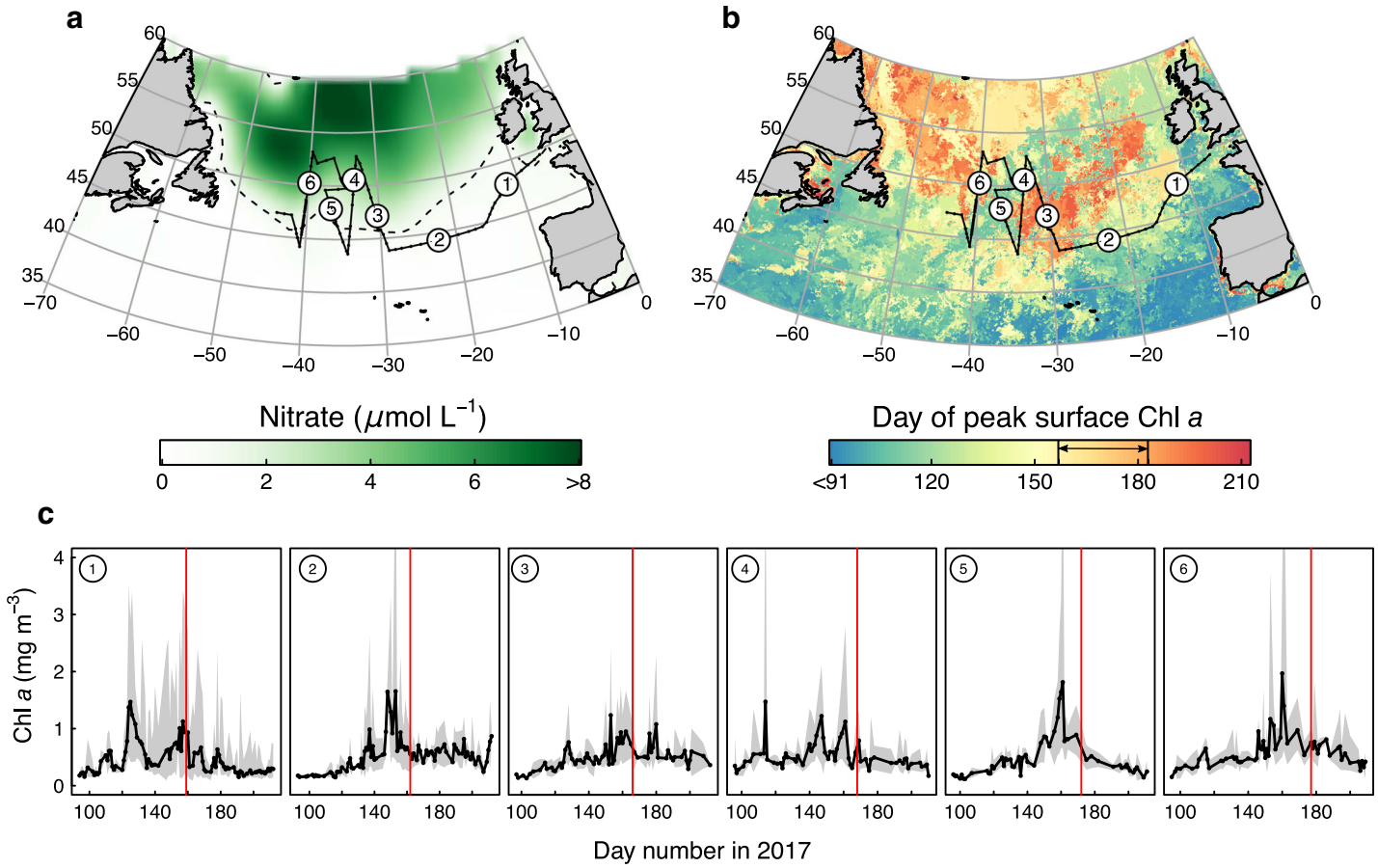

Fig. 1. Locations of cruise track and experiments in context of the regional nitrate gradient and bloom stage. (**a**) Background of World Ocean Atlas nitrate (interpolated for June); solid line = cruise transect; dashed line = 1 μmol L^{-1} nitrate contour. (**b**) Background of peak Chl *a* day number in 2017, indicating basin-scale bloom progression (timing of study cruise is indicated; day numbers 157–183). (**c**) Experimental timing in relation to satellite-derived spring–summer surface Chl *a*. Data are for a 3 × 3° box around experimental sites; solid line = mean, shading = range. Vertical red lines indicate experimental start days.

maximum fluorescence (F_m). Blank fluorescence was determined on 0.2 μm filtrates and was subtracted from F_o and F_m before calculation of $F_v/F_m = (F_m - F_o)/F_m$.

Results and discussion

Occupation in relation to bloom timing

Satellite observations indicated that the ship-board experiments were conducted around, or post, peak springtime surface Chl *a* concentrations, confirming bloom climax or postbloom conditions (Fig. 1b,c).

Limitation by iron and/or nitrogen

Plankton biomass (POC) accumulated and nitrate was drawn down in untreated control bottles at all experimental sites apart from Experiment 2 where POC decreased (Fig. 2; Table 1). Given that in situ light availability was expected to be replete (i.e., critical depths > mixed layer depths; Siegel et al. 2002), this implied plankton loss processes were reduced upon incubation (i.e., via grazing, viral lysis, dispersal), therefore allowing net plankton accumulation independent of changes in phytoplankton specific growth rates (e.g., Cullen 1991; Banse 2002; Behrenfeld and Boss 2018). However, following experimental supply of either fixed N (Experiments 1–2) or Fe (Experiments 3–6), Chl *a* and POC concentrations increased significantly beyond untreated controls (Fig. 2a–l). Alongside coregulation by loss processes, these responses therefore provided evidence for N or Fe limitation of the overall phytoplankton yield at all experimental sites (i.e., Liebig limitation; de Baar 1994). Furthermore, provided phytoplankton losses did not differ between treatments (i.e., via differences in grazing rates), these responses also suggested nutrient limitation of the community-level specific growth rate (i.e., Blackman limitation; Cullen 1991; de Baar 1994; Moore et al. 2013).

The geographic pattern of responses to N and Fe supply in relation to the regional nitrate gradient was consistent with previous studies in the North Atlantic (Fig. 1a). Collectively, these studies have suggested a transition from Fe limitation at higher

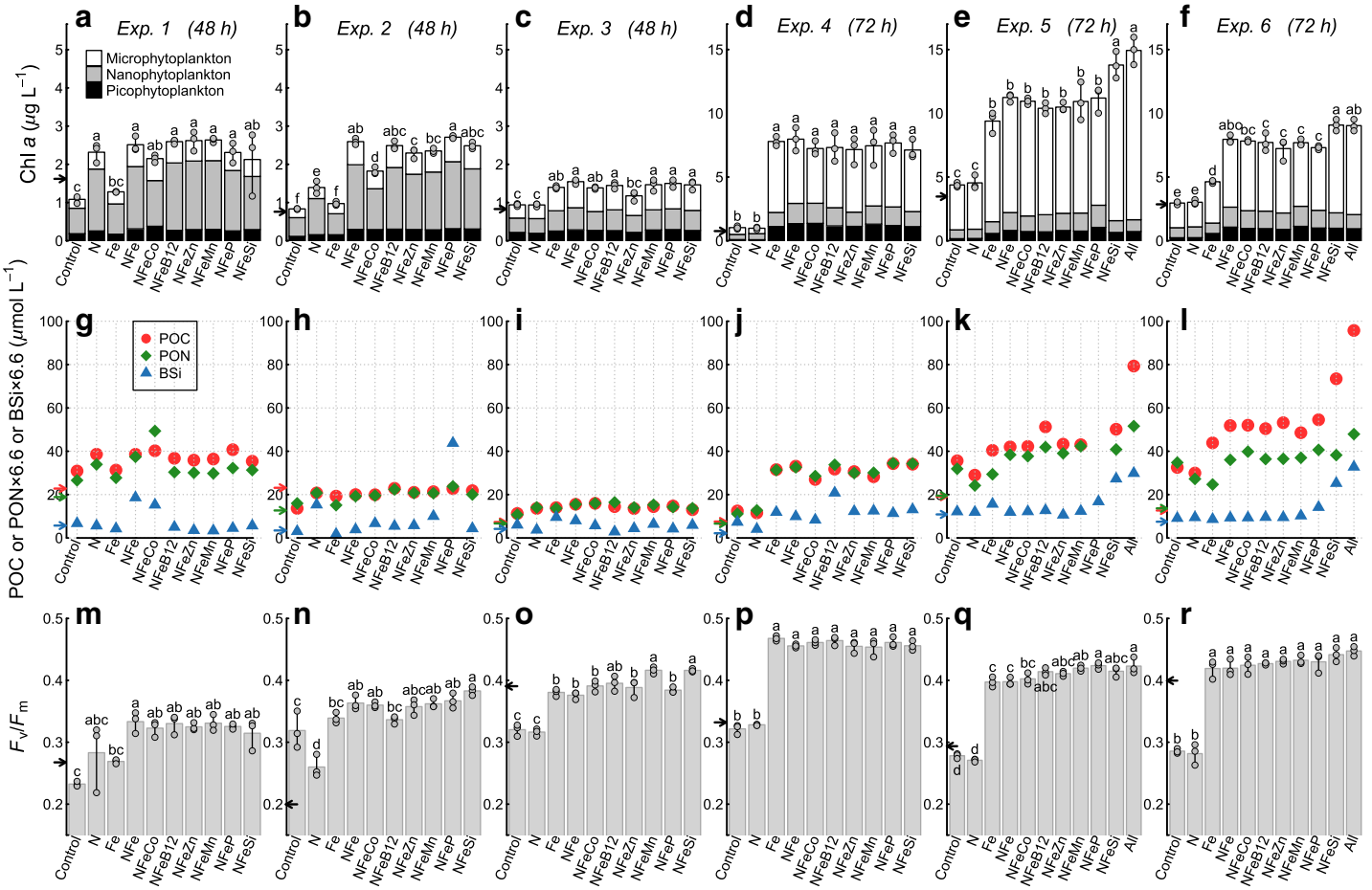

Fig. 2. Phytoplankton responses to nutrient supply. (**a**–**f**) Mean Chl *a* responses (bar heights; $n = 3$), with replicate values indicated (gray dots). Note the change in y-axis scaling between panels (**a**–**c**) and (**d**–**f**). Bar shading indicates the fractional contribution of different size groups to total Chl *a* (Uitz et al. 2006). (**g**–**l**) POC, PON, and BSi responses ($n = 1$). (**m**–**r**) Mean F_v/F_m responses (bar heights; $n = 3$), with replicate values indicated (gray dots). For all panels, arrows point to initial conditions. For panels (**a**–**f**) and (**m**–**r**), bars labeled with different letters indicate significantly different means (ANOVA $p < 0.05$ followed by a Tukey honesty significant difference test).

latitudes in spring/summer (which host residual nitrate; Fig. 1a), to year-round N limitation in the subtropical gyre to the south (Graziano et al. 1996; Blain et al. 2004; Moore et al. 2006, 2008; Nielsdóttir et al. 2009; Ryan-Keogh et al. 2013). Accordingly, transitions in the primary limiting nutrients, between either N or Fe, were in turn predictable on the basis of the initial concentrations of nitrate alone, the dissolved ratio of nitrate to Fe (i.e., N:Fe), or calculated values of Fe* (see Table 1; Browning et al. 2014, 2017, 2018; Moore 2016). Conditions approaching N-Fe co-limitation were also apparent in Experiments 2 and 6 (Fig. 2b,f; Browning et al. 2017; Ryan-Keogh et al. 2013). Specifically, serial Chl *a* responses observed following N + Fe supply were significantly higher than those following the supply of the primary limiting nutrient alone.

Community-level photophysiological responses to nutrient supply, in terms of the apparent PSII photochemical efficiency (F_v/F_m) and functional absorption cross section (σ_{PSII}), also exhibited a marked transition between N- and Fe-limited regimes (Fig. 2m–r; Table 1). F_v/F_m showed significant increases following Fe addition relative to controls at Fe-limited sites (Experiments 3–6) and restricted changes following N or Fe addition at N-limited sites (Experiments 1–2). σ_{PSII} responded with changes inverse to F_v/F_m, with the two parameters negatively correlated across the experimental dataset ($R^2 = 0.76$, $p < 1 \times 10^{-15}$, $n = 192$). These responses are consistent with prior observations, likely regulated by a mechanism involving phytoplankton accumulating fluorescent light harvesting complexes that are energetically decoupled from PSII under Fe limited, N sufficient conditions (leading to low F_v/F_m) and their rapid connection to an increasing PSII pool following Fe supply (increasing F_v/F_m and decreasing σ_{PSII}) (Behrenfeld et al. 2006; Moore et al. 2006; Schrader et al. 2011; Behrenfeld and Milligan 2013; Ryan-Keogh et al. 2013; Browning et al. 2014; Macey et al. 2014; Browning et al. 2017; Li et al. 2019; Schoffman and Keren 2019).

Community response to supply of limiting nutrients

In the shorter duration experiments in the eastern portion of the cruise track (Experiments 1–3; Table 1; Fig. 1),

Table 1. Initial conditions, responses, and limiting nutrients in bioassay experiments.

	Exp. 1	Exp. 2	Exp. 3	Exp. 4	Exp. 5	Exp. 6
Incubation duration (h)	~48	~48	~48	~72	~72	~72
Longitude (°E)	−11.7	−22.4	−30.3	−33.4	−36.7	−39.9
Latitude (°N)	47.9	44.3	47.2	50.6	47.9	50.2
Initial temperature (°C)	15.0	16.5	15.7	12.9	14.3	12.3
MLD	—	—	17.0	13.5	16.7	16.9
Nitrate (μmol L^{-1})	0.18	0.41	3.15	6.12	2.91	2.47
Phosphate (μmol L^{-1})	0.09	0.05	0.16	0.37	0.17	0.18
Silicic acid (μmol L^{-1})	0.38	0.94	1.37	2.66	0.14	0.29
DFe (nmol L^{-1})	0.25	0.44	0.14	0.31	0.37	0.20
Chl *a* (μg L^{-1})	1.62	0.76	0.83	0.76	3.47	2.86
POC (μmol L^{-1})	22.8	23.14	7.34	7.57	19.05	12.66
BSi (μmol L^{-1})	0.86	0.52	0.63	0.33	1.64	1.13
Initially dominant phytoplankton size fraction	Nano	Nano	Nano/micro	Nano/micro	Micro	Micro
Log_{10} (N:Fe)	−0.14	−0.03	1.36	1.29	0.90	1.09
Fe_N* nmol L^{-1}	0.17	0.25	−1.34	−2.56	−0.99	−0.96
F_v/F_m (+Fe) − F_v/F_m (C)	0.04	0.02	0.06†	0.15†	0.12†	0.13†
Final nitrate (μmol L^{-1})						
Control	<0.08	<0.08	1.56	4.52	0.65	0.10
N + Fe	<0.08	0.31	3.72	1.91	0.13	<0.08
Limiting nutrient‡	N	N(Fe)	Fe	Fe	Fe	Fe(N)

Fe_N* represents the dissolved Fe concentration in excess of assumed-average phytoplankton N requirements, $Fe_N^* = Fe - R_{Fe:N} \times N$, where Fe and N are the respective dissolved concentrations in seawater and $R_{Fe:N}$ is the assumed average Fe:N stoichiometry of phytoplankton (0.469×10^{-3} mol:mol from Moore et al. 2013), MLD: mixed layer depth.

†Statistically significant increase in F_v/F_m in +Fe treatments relative to control (C) (ANOVA $p < 0.05$ followed by a Tukey honesty significant difference test across all treatments).

‡Elements in brackets indicates secondary limiting nutrients.

phytoplankton appeared to be initially dominated by nanophytoplankton, which, matching bulk Chl *a* responses, generally increased in number and intracellular Chl *a* content following N and/or Fe supply relative to untreated controls (Figs. 2a–c, 3a–c). The initial situation of few larger cells at these sites, including low diatom abundance (*see* Supporting Information), together with relatively short incubation timescales (~ 48 h), collectively appeared to restrict both large absolute increases in phytoplankton biomass and accompanying changes in the size structure of phytoplankton communities following nutrient amendment (e.g., Chisholm 1992; Price et al. 1994). Conversely, the longer duration experiments (Experiments 4–6; Table 1) were initially codominated by nano- and microphytoplankton, with a greater abundance of diatoms (Fig. 2d–f; Supporting Information). At these sites, amendment with limiting nutrients (Fe or Fe + N) also enhanced abundances of pico- and nanophytoplankton (Barber and Hiscock 2006), but increases in microphytoplankton fractions were much larger, matching Chl *a* and POC biomass accumulation (Figs. 2d–f, 3d–f). Greater contributions of the pigment fucoxanthin (data not shown) suggested that the enhanced biomass was attributable to diatoms. This was confirmed by increased dominance of large *Thalassionemataceae* colonies and *Guinardia* chains (~ 100s μm length) in microscopy samples, which were much less common in controls (with the latter diatom assemblage mostly comprising smaller [~ 10s μm] individual *Pseudo-nitzschia* cells; *see* Supporting Information).

The responses observed in Experiments 4–6 suggested that the pre-existing larger celled diatom community was experiencing greater Fe limitation in situ than the smaller celled community (Cullen 1991; Price et al. 1994; Ryan-Keogh et al. 2013). Following Fe supply however, adaptations enabling higher maximum potential growth rates (Marañón et al. 2012), rapid uptake and storage of nutrients under conditions of high nutrient availability (Raven 1987; Marchetti et al. 2009, 2012), together with lower susceptibility to grazer control (Smetacek 1999), presumably enabled their disproportionate accumulation and the accompanying drawdown of available nitrate (Table 1; de Baar et al. 2005).

Minimal individual limitation by Si, P, Co, vitamin B_{12}, Zn, or Mn

No clear serial biomass responses to any of the additional (micro)nutrients (P, Si, Mn, Co, Zn, B_{12}), supplied in combination with N + Fe, were observed in Experiments 1–4. This suggested that these nutrients were not deficient enough in the ambient seawater, nor the incubated seawater supplemented

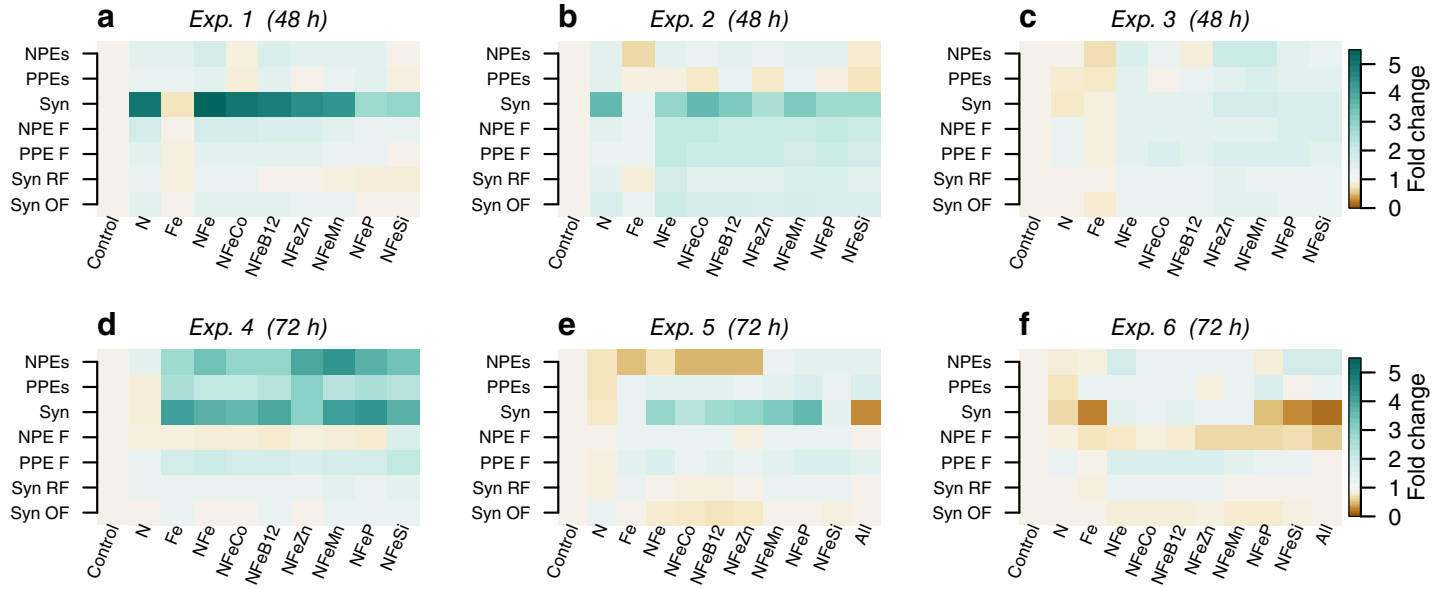

Fig. 3. Community-specific responses to nutrient supply. Heat maps indicate fold changes in flow cytometry-derived cell properties following nutrient amendment relative to unamended controls (NPE, nano-photosynthetic eukaryotes; PPE, pico-photosynthetic eukaryotes; Syn, *Synechococcus*; F, cellular fluorescence, RF, red fluorescence; OR, orange fluorescence).

with N + Fe, to markedly restrict phytoplankton accumulation over experimental timescales. In contrast, in Experiments 5 and 6 small additional Chl *a* enhancements were observed upon supply of N + Fe + Si (Fig. 2e,f). This indicated that serial Si limitation could have restricted diatom growth rates and/or susceptibility to grazing following supply of N + Fe alone. Indeed, assuming typical phytoplankton elemental quotas and diatom Si requirements (reported in Moore et al. 2013), initial silicic acid concentrations were more deficient than either Fe or N in the initial seawater (not shown). However, the substantial Chl *a* and diatom accumulation that was observed following supply of Fe + N alone (2.6- and 2.7-fold Chl *a* increases relative to controls in Experiments 5 and 6, respectively; initial Si < 0.3 μmol L^{-1}; see also Supporting Information), implied that Si availability—as for the other non-N or Fe nutrients tested—was not a primary limiting factor in situ (Rynearson et al. 2013). This could potentially be reconciled with a high degree of plasticity in Si requirements: despite the large biomass changes, BSi concentrations were largely invariant between Fe(+N) amendments and controls (Fig. 2). This may in turn have been related to either shifts toward less silicified diatom species (Assmy et al. 2013; Smetacek 2018) and/or reductions in silicification following Fe supply (Hutchins and Bruland 1998; Takeda 1998).

Multiple nutrient supply and non-Redfield POC accumulation

While having relatively little extra impact on Chl *a* responses, supply of all eight nutrients in combination appeared to have an important influence on POC accumulation at the two sites where this treatment was conducted. In Experiments 5 and 6, Chl *a* in this treatment was not enhanced relative to the Fe + N + Si treatment, but POC was enhanced a further 1.3-fold (Experiment 5) and 1.6-fold (Experiment 6) (Fig. 2e,f). These POC increases were not matched by an equivalent PON enhancement in Redfield proportions (C:N > 10 compared to Redfield C:N of 6.6).

Such postbloom "carbon overconsumption" likely reflects diatom response to exhaustion of dissolved inorganic N (the starting seawater concentration + that artificially supplied; Toggweiler 1993; Körtzinger et al. 2001; Engel et al. 2002; Wetz and Wheeler 2003; Riebesell et al. 2007; Taucher et al. 2012). However, near-full nitrate depletion over the 72 h experiment duration was already apparent in the N + Fe treatments (and while not measured, presumably also in +Fe; Table 1), which did not yield such high POC (or POC:PON). Furthermore, F_v/F_m remained elevated in all "+Fe" treatments, demonstrating phytoplankton were not N-starved (Geider et al. 1993; Parkhill et al. 2001). Together this suggested that while N depletion was probably a necessary condition for the elevated POC:PON, it alone could not explain the large differences between treatments.

Numerous biochemical dependencies exist that could link provision of (micro)nutrients not directly restricting (N-limited) Chl *a* synthesis with enhanced photosynthate production (Morel and Price 2003; Saito et al. 2008). We can only speculate as to their relative importance. For instance, under conditions of high carbon fixation, the rate of inorganic carbon acquisition may be constrained by carbonic anhydrase activity, which itself might depend on the availability of activating Zn, Co, or Cd cofactors (Riebesell et al. 1993; Morel et al. 1994; Cullen et al. 1999). Likewise, vitamin B_{12} catalyzes a variety of carbon metabolism and might not always be sufficiently available to maximize the rates of these reactions (Bertrand and Allen 2012; Bertrand et al. 2015).

Implications for carbon export

The different POC:PON accumulation between N + Fe and "all" nutrient combinations could have important implications for our understanding of the way that phytoplankton blooms are regulated in natural systems. The "additional" C in the multinutrient treatments was likely channeled into production and exudation of C-rich, N-poor molecules into phycospheres of the dominant large diatoms (Seymour et al. 2017). In turn, this could potentially be related to stimulation of bacterial phycosphere colonization, which could increase production of enzymes liberating nutrients from dissolved organic pools and/or the synthesis of scarce vitamins (Bertrand and Allen 2012; Bertrand et al. 2015; Seymour et al. 2017). Regardless of why this occurs, in natural systems such sticky exudates coagulate into gel-like particles (Engel 2004; Verdugo et al. 2004; Engel et al. 2015), enhance particle aggregation, and speed up sinking of the high C:N organic material in the water column (Smetacek 1985; Passow and Alldredge 1994; Engel et al. 2002; Martin et al. 2011). Multinutrient regulation of sticky organic exudate production could therefore represent a link between (1) the simultaneous availability of multiple resources as N becomes depleted and (2) export efficiency of diatom blooms to the deep ocean (Billett et al. 1983; Rynearson et al. 2013; Agustí et al. 2015).

Conclusions

Our experiments suggested spatial transitions in primary limitation of phytoplankton by either Fe or fixed N throughout the mid-latitude North Atlantic in late spring. This accords with results from previous studies elsewhere in the North Atlantic (Blain et al. 2004; Moore et al. 2006; Nielsdóttir et al. 2009; Ryan-Keogh et al. 2013). Transitions in limiting nutrients fit within an overall seasonal shift in the bottom-up resource controls on phytoplankton growth (Ryan-Keogh et al. 2013): from early season light limitation, transitioning to Fe limitation, and subsequently, N limitation where winter mixed layer nitrate inventories are lower and/or Fe supply is higher (Moore et al. 2006; Achterberg et al. 2013; Ryan-Keogh et al. 2013; Achterberg et al. 2018; Hopwood et al. 2018; Sedwick et al. 2018; Birchhill et al. 2019). In combination with top-down grazer control, either or both nutrients could therefore sufficiently slow growth rates of larger phytoplankton to terminate the spring bloom (Banse 2002; Ryan-Keogh et al. 2013; Behrenfeld and Boss 2018). Substantial chlorophyll and diatom accumulation occurred following Fe + N supply, with or without provision of supplementary (micro) nutrients (Si, P, Mn, Co, Zn, B_{12}). This implied that the latter were not primary factors limiting bloom formation at the timescales (48–72 h) of our bioassay experiments. We infer that they do not terminate the spring bloom in situ either. However, simultaneous supply of multiple nutrients did lead to enhanced POC production, suggesting multinutrient availability might be important for maximizing transient carbon export, particularly if the additional POC included sticky exudates that enhance cell aggregation and accelerate sinking (Smetacek 1985; Passow and Alldredge 1994; Engel et al. 2002, 2015; Engel 2004; Verdugo et al. 2004; Martin et al. 2011).

These observations have raised a number of further questions. First, the critical nutrient combinations have been constrained, but not fully resolved. Exactly which combinations of nutrients, in addition to Fe + N + Si, would produce the responses triggered when all eight were supplied together (Fig. 2e,f)? Our results imply the required (micro)nutrients—or at least those with differing sources, sinks and seawater chemistries—would have to be considered to accurately predict POC accumulation and its corresponding C:N ratio (Schartau et al. 2007). Second, is the high POC:PON ratio of particulate organic matter linked to transient phytoplankton blooming and carbon export? Exudation of high C:N organic matter is predicted to enhance particle abundance, aggregation, and sinking (Engel 2004; Engel et al. 2004). This would lead to faster and more efficient export of phytoplankton carbon because of (1) more rapid transfer of fixed carbon below the thermocline prior to remineralization, and (2) more carbon export per utilized N (Geider et al. 2001; Engel et al. 2004).

The short timescales that might be associated with high C:N diatom blooming and export (days–weeks; e.g., Billett et al. 1983; Lochte et al. 1993; Dale et al. 1999; Mahadevan et al. 2012; Riley et al. 2012; Rynearson et al. 2013; Agustí et al. 2015; Smith et al. 2018), severely complicates efforts to detect and observe these events, if they occur naturally, with either conventional ocean observation programs (e.g., Goldman 1993) or indirectly via remote satellite observations (the latter having a resolution that is generally too low at the relevant time scales; Kahru 2017). Planned multidisciplinary observational programs including autonomous field platforms, which are specifically designed to capture high spatial and temporal variability, might be able to overcome this (Sanders et al. 2016; Siegel et al. 2016; Behrenfeld et al. 2019; Boyd et al. 2019).

References

Achterberg, E. P., and others. 2013. Natural iron fertilization by the Eyjafjallajokull volcanic eruption. Geophys. Res. Lett. **40**: 921–926. doi:10.1002/grl.50221

Achterberg, E. P., and others. 2018. Iron biogeochemistry in the high latitude North Atlantic Ocean. Sci. Rep. **8**: 1283. doi:10.1038/s41598-018-19472-1

Agustí, S., J. I. González-Gordillo, D. Vaqué, M. Estrada, M. I. Cerezo, G. Salazar, J. M. Gasol, and C. M. Duarte. 2015. Ubiquitous healthy diatoms in the deep sea confirm deep carbon injection by the biological pump. Nat. Commun. **6**: 7608. doi:10.1038/ncomms8608

Alldredge, A. L., and C. C. Gotschalk. 1989. Direct observations of the mass flocculation of diatom blooms: Characteristics, settling velocities and formation of diatom aggregates.

Deep-Sea Res. A **36**: 159–171. doi:10.1016/0198-0149(89)90131-3

Allen, J. T., and others. 2005. Diatom carbon export enhanced by silicate upwelling in the Northeast Atlantic. Nature **437**: 728–732. doi:10.1038/nature03948

Assmy, P. et al. 2013. Thick-shelled, grazer-protected diatoms decouple ocean carbon and silicon cycles in the iron-limited Antarctic Circumpolar Current. Proc. Natl. Acad. Sci. **110**: 20633–20638. doi:10.1073/pnas.1309345110

Banse, K. 2002. Steemann Nielsen and the zooplankton. Hydrobiologia **480**: 15–28. doi:10.1023/A:1021220714899

Barber, R. T., and M. R. Hiscock. 2006. A rising tide lifts all phytoplankton: Growth response of other phytoplankton taxa in diatom-dominated blooms. Global Biogeochem. Cycles **20**: GB4S03. doi:10.1029/2006GB002726

Barlow, R. G., R. F. C. Mantoura, M. A. Gough, and T. W. Fileman. 1993. Pigment signatures of the phytoplankton composition in the northeastern Atlantic during the 1990 spring bloom. Deep-Sea Res. II Top. Stud. Oceanogr. **40**: 459–477. doi:10.1016/0967-0645(93)90027-K

Behrenfeld, M. J., K. Worthington, R. M. Sherrell, F. P. Chavez, P. Strutton, M. McPhaden, and D. M. Shea. 2006. Controls on tropical Pacific Ocean productivity revealed through nutrient stress diagnostics. Nature **442**: 1025–1028. doi:10.1038/nature05083

Behrenfeld, M. J., and A. J. Milligan. 2013. Photophysiological expressions of iron stress in phytoplankton. Ann. Rev. Mar. Sci. **5**: 217–246. doi:10.1146/annurev-marine-121211-172356

Behrenfeld, M. J., and E. S. Boss. 2018. Student's tutorial on bloom hypotheses in the context of phytoplankton annual cycles. Glob. Chang. Biol. **24**: 55–77. doi:10.1111/gcb.13858

Behrenfeld, M. J., and others. 2019. The North Atlantic Aerosol and Marine Ecosystem Study (NAAMES): Science motive and mission overview. Front. Mar. Sci. **6**: 22. doi:10.3389/fmars.2019.00122

Bertrand, E. M., and A. E. Allen. 2012. Influence of vitamin B auxotrophy on nitrogen metabolism in eukaryotic phytoplankton. Front. Microbiol. **3**: 375. doi:10.3389/fmicb.2012.00375

Bertrand, E. M., and others. 2015. Phytoplankton-bacterial interactions mediate micronutrient colimitation at the coastal Antarctic Sea ice edge. Proc. Natl. Acad. Sci. USA **112**: 9938–9943. doi:10.1073/pnas.1501615112

Billett, D. S. M., R. S. Lampitt, A. L. Rice, and R. F. C. Mantoura. 1983. Seasonal sedimentation of phytoplankton to the deep-sea benthos. Nature **302**: 520–522. doi:10.1038/302520a0

Birchill, A.J., N. T. Hartner, K. Kunde, B. Siemering, C. Daniels, D. Gonzalez-Santana, A. Milne, S. J. Ussher, P. J. Worsfold, K. Leopold, and S. C., Painter, 2019. The eastern extent of seasonal iron limitation in the high latitude North Atlantic Ocean. Sci. Rep. **9**: 1435. doi:10.1038/s41598-018-37436-3

Blain, S., C. Guieu, H. Claustre, K. Leblanc, T. Moutin, B. Quéguiner, J. Ras, and G. Sarthou. 2004. Availability of iron and major nutrients for phytoplankton in the northeast Atlantic Ocean. Limnol. Oceanogr. **49**: 2095–2104. doi:10.4319/lo.2004.49.6.2095

Boyd, P. W., H. Claustre, M. Lévy, D. A. Siegel, and T. Weber. 2019. Multi-faceted particles pumps drive carbon sequestration in the ocean. Nature **568**: 327–335. doi:10.1038/s41586-019-1098-2

Browning, T. J., H. A. Bouman, C. M. Moore, C. Schlosser, G. A. Tarran, E. M. S. Woodward, and G. M. Henderson. 2014. Nutrient regimes control phytoplankton ecophysiology in the South Atlantic. Biogeosciences **11**: 463–479. doi:10.5194/bg-11-463-2014

Browning, T. J., E. P. Achterberg, I. Rapp, A. Engel, E. M. Bertrand, A. Tagliabue, and C. M. Moore. 2017. Nutrient co-limitation at the boundary of an oceanic gyre. Nature **551**: 242–246. doi:10.1038/nature24063

Browning, T.J., I. Rapp, C. Schlosser, M. Gledhill, E. P. Achterberg, A. Bracher, and F. A. Le Moigne, 2018. Influence of iron, cobalt, and vitamin B12 supply on phytoplankton growth in the tropical East Pacific during the 2015 El Niño. Geophys. Res. Lett. **45**: 6150–6159. doi:10.1029/2018GL077972

Buesseler, K. O., M. P. Bacon, J. K. Cochran, and H. D. Livingston. 1992. Carbon and nitrogen export during the JGOFS North Atlantic Bloom experiment estimated from ^{234}Th: ^{238}U disequilibria. Deep-Sea Res. A **39**: 1115–1137. doi:10.1016/0198-0149(92)90060-7

Buesseler, K. O., and P. W. Boyd. 2009. Shedding light on processes that control particle export and flux attenuation in the twilight zone of the open ocean. Limnol. Oceanogr. **54**: 1210–1232. doi:10.4319/lo.2009.54.4.1210

Chisholm, S. W. 1992. Phytoplankton size, p. 213–237. *In* P. G. Falkowski, A. D. Woodhead and K. Vivirito [eds.], Primary productivity and biogeochemical cycles in the sea. Springer.

Cullen, J. J. 1991. Hypotheses to explain high-nutrient conditions in the open sea. Limnol. Oceanogr. **36**: 1578–1599. doi:10.4319/lo.1991.36.8.1578

Cullen, J.T., T. W. Lane, F. M. Morel, and R. M. Sherrell, 1999. Modulation of cadmium uptake in phytoplankton by seawater CO2 concentration. Nature, **402**: 165–167. doi:10.1038/46007

Dale, T., F. Rey, and B. R. Heimdal. 1999. Seasonal development of phytoplankton at a high latitude oceanic site. Sarsia **84**: 419–435. doi:10.1080/00364827.1999.10807347

Daniels, C. J., A. J. Poulton, M. Esposito, M. L. Paulsen, R. Bellerby, M. St John, and A. P. Martin. 2015. Phytoplankton dynamics in contrasting early stage North Atlantic spring blooms : Composition, succession, and potential drivers. Biogeosciences **12**: 2395–2409. doi:10.5194/bg-12-2395-2015

Davey, M., G. A. Tarran, M. M. Mills, C. Ridame, R. J. Geider, and J. LaRoche. 2008. Nutrient limitation of picophytoplankton photosynthesis and growth in the tropical

North Atlantic. Limnol. Oceanogr. **53**: 1722–1733. doi:10.4319/lo.2008.53.5.1722

de Baar, H. J. W. 1994. von Liebig's law of the minimum and plankton ecology (1899–1991). Prog. Oceanogr. **33**: 347–386. doi:10.1016/0079-6611(94)90022-1

de Baar, H. J. W., and others. 2005. Synthesis of iron fertilization experiments: From the iron age in the age of enlightenment. J. Geophys. Res. Oceans **110**: C09S16. doi:10.1029/2004JC002601

Ellwood, M. J., and C. M. van den Berg. 2000. Zinc speciation in the northeastern Atlantic Ocean. Mar. Chem. **68**: 295–306. doi:10.1016/S0304-4203(99)00085-7

Ellwood, M. J., and C. M. van den Berg. 2001. Determination of organic complexation of cobalt in seawater by cathodic stripping voltammetry. Mar. Chem. **75**: 33–47. doi:10.1016/S0304-4203(01)00024-X

Engel, A. 2004. Distribution of transparent exopolymer particles (TEP) in the Northeast Atlantic Ocean and their potential significance for aggregation processes. Deep-Sea Res. Part I Oceanogr. Res. Pap. **51**: 83–92. doi:10.1016/j.dsr.2003.09.001

Engel, A., S. Goldthwait, U. Passow, and A. Alldredge. 2002. Temporal decoupling of carbon and nitrogen dynamics in a mesocosm diatom bloom. Limnol. Oceanogr. **47**: 753–761. doi:10.4319/lo.2002.47.3.0753

Engel, A., S. Thoms, U. Riebesell, E. Rochelle-Newall, and I. Zondervan. 2004. Polysaccharide aggregation as a potential sink of marine dissolved organic carbon. Nature **428**: 929–932. doi:10.1038/nature02453

Engel, A., C. Borchard, A. Loginova, J. Meyer, H. Hauss, and R. Kiko. 2015. Effects of varied nitrate and phosphate supply on polysaccharidic and proteinaceous gel particle production during tropical phytoplankton bloom experiments. Biogeosciences **12**: 5647–5665. doi:10.5194/bg-12-5647-2015

Geider, R. J., J. La Roche, R. M. Greene, and M. Olaizola. 1993. Response of the photosynthetic apparatus of *Phaeodactylum tricornatum* (Bacillariophycea) to nitrate, phosphate, or iron starvation. J. Phycol. **29**: 755–766. doi:10.1111/j.0022-3646.1993.00755.x

Geider, R. J., and others. 2001. Primary productivity of planet earth: Biological determinants and physical constraints in terrestrial and aquatic habitats. Glob. Chang. Biol. **7**: 849–882. doi:10.1046/j.1365-2486.2001.00448.x

Goldman, J. C. 1993. Potential role of large oceanic diatoms in new primary production. Deep-Sea Res. Part I Oceanogr. Res. Pap. **40**: 159–168. doi:10.1016/0967-0637(93)90059-C

Graziano, L. M., R. J. Geider, W. K. W. Li, and M. Oloaizola. 1996. Nitrogen limitation of North Atlantic phytoplankton: Analysis of physiological condition in nutrient enrichment experiments. Aquat. Microb. Ecol. **11**: 53–64. doi:10.3354/ame011053

Henson, S. A., R. Sanders, C. Holeton, and J. T. Allen. 2006. Timing of nutrient depletion, diatom dominance and a lower- boundary estimate of export production for Irminger Basin, North Atlantic. Mar. Ecol. Prog. Ser. **313**: 73–84. doi:10.3354/meps313073

Hopwood, M. J., D. Carroll, T. J. Browning, L. Meire, J. Mortensen, S. Krisch, and E. P. Achterberg. 2018. Non-linear response of summertime marine productivity to increased meltwater discharge around Greenland. Nat. Commun. **9**: 3256. doi:10.1038/s41467-018-05488-8

Hutchins, D. A., and K. W. Bruland. 1998. Iron-limited diatom growth and Si:N uptake ratios in a coastal upwelling regime. Nature **393**: 561–564. doi:10.1038/31203

Kahru, M. 2017. Ocean productivity from space: Commentary. Global Biogeochem. Cycles **31**: 214–216. doi:10.1002/2016GB005582

Kolber, Z. S., O. Prášil, and P. G. Falkowski. 1998. Measurements of variable chlorophyll fluorescence using fast repetition rate techniques: Defining methodology and experimental protocols. Biochim. Biophys. Acta **1367**: 88–106. doi:10.1016/S0005-2728(98)00135-2

Körtzinger, A., W. Koeve, P. Kahler, and L. Mintrop. 2001. C:N ratios in the mixed layer during the productive season in the Northeast Atlantic Ocean. Deep-Sea Res. Part I Oceanogr. Res. Pap. **48**: 661–688. doi:10.1016/S0967-0637(00)00051-0

Körtzinger, A., and others. 2008. The seasonal pCO_2 cycle at 49 N/16.5 W in the northeastern Atlantic Ocean and what it tells us about biological productivity. J. Geophys. Res. Oceans **113**: C04020.

Lampitt, R. S. 1985. Evidence for the seasonal deposition of detritus to the deep-sea floor and its subsequent resuspension. Deep-Sea Res. A **32**: 885–897. doi:10.1016/0198-0149(85)90034-2

Leblanc, K., and others. 2009. Distribution of calcifying and silicifying phytoplankton in relation to environmental and biogeochemical parameters during the late stages of the 2005 North East Atlantic Spring Bloom. Biogeosciences **6**: 2155–2179. doi:10.5194/bg-6-2155-2009

Lochte, K., H. W. Ducklow, M. J. R. Fasham, and C. Stienen. 1993. Plankton succession and carbon cycling at 47 N 20 W during the JGOFS North Atlantic Bloom Experiment. Deep-Sea Res. Part II Top. Stud. Oceanogr. **40**: 91–114. doi:10.1016/0967-0645(93)90008-B

Li, Q., J. Huisman, T. S. Bibby, and N. Jiao. 2019. Biogeography of Cyanobacterial isiA Genes and Their Link to Iron Availability in the Ocean. Front. Microbiol. **10**: 650. doi:10.3389/fmicb.2019.00650

Macey, A.I., T. Ryan-Keogh, S. Richier, C. M. Moore, and T. S. Bibby, 2014. Photosynthetic protein stoichiometry and photophysiology in the high latitude North Atlantic. Limnol. Oceanogr. **59**: 1853–1864. doi:10.4319/lo.2014.59.6.1853

Mahadevan, A., E. D'Asaro, C. Lee, and M. J. Perry. 2012. Eddy-driven stratification initiates North Atlantic spring phytoplankton blooms. Science **337**: 54–58. doi:10.1371/journal.pone.0051845

Marchetti, A., and others. 2009. Ferritin is used for iron storage in bloom-forming marine pennate diatoms. Nature **457**: 467–470. doi:10.1038/nature07539

Marchetti, A., and others. 2012. Comparative metatranscriptomics identifies molecular bases for the physiological responses of phytoplankton to varying iron availability. Proc. Natl. Acad. Sci. USA **109**: 317–325. doi:10.1073/pnas.1118408109

Martin, P., R. S. Lampitt, M. J. Perry, R. Sanders, C. Lee, and E. D'Asaro. 2011. Export and mesopelagic particle flux during a North Atlantic spring diatom bloom. Deep-Sea Res. Part I Oceanogr. Res. Pap. **58**: 338–349. doi:10.1016/j.dsr.2011.01.006

Maranón, E., P. Cermeno, M. Latasa, and R. D. Tadonléké, 2012. Temperature, resources, and phytoplankton size structure in the ocean. Limnol. Oceanogr. **57**: 1266–1278. doi:10.4319/lo.2012.57.5.1266

Moore, C. M. et al. 2013. Processes and patterns of oceanic nutrient limitation, Nat. Geosci., **6**: 701–710. doi:10.1038/ngeo1765

Mignot, A., R. Ferrari, and H. Claustre. 2018. Floats with bio-optical sensors reveal what processes trigger the North Atlantic bloom. Nat. Commun. **9**: 190. doi:10.1038/s41467-017-02143-6

Montegut, C. D., G. Madec, A. S. Fischer, A. Lazar, and D. Iudicone. 2004. Mixed layer depth over the global ocean: An examination of profile data and a profile-based climatology. J. Geophys. Res. Oceans **109**: C102003. doi:10.1029/2004JC002378

Moore, C. M. 2016. Diagnosing oceanic nutrient deficiency. Philos. Trans. R. Soc. A Math. Phys. Eng. Sci. **374**: 20150290. doi:10.1098/rsta.2015.0290

Moore, C. M., M. I. Lucas, R. Sanders, and R. Davidson. 2005. Basin-scale variability of phytoplankton bio-optical characteristics in relation to bloom state and community structure in the Northeast Atlantic. Deep-Sea Res. Part I Oceanogr. Res. Pap. **52**: 401–419. doi:10.1016/j.dsr.2004.09.003

Moore, C. M., M. M. Mills, A. Milne, R. Langlois, E. P. Achterberg, K. Lochte, R. J. Geider, and J. La Roche. 2006. Iron limits primary productivity during spring bloom development in the central North Atlantic. Glob. Chang. Biol. **12**: 626–634. doi:10.1111/j.1365-2486.2006.01122.x

Moore, C. M., and others. 2008. Relative influence of nitrogen and phosphorus availability on phytoplankton physiology and productivity in the oligotrophic sub-tropical North Atlantic Ocean. Limnol. Oceanogr. **53**: 824–834. doi:10.4319/lo.2008.53.1.0291

Morel, F. M. M., J. R. Reinfelder, S. B. Roberts, C. P. Chamberlain, J. G. Lee, and D. Yee. 1994. Zinc and carbon co-limitation of marine phytoplankton. Nature **369**: 740–742. doi:10.1038/369740a0

Morel, F. M. M., and N. M. Price. 2003. The biogeochemical cycles of trace metals in the oceans. Science **300**: 944–947. doi:10.1126/science.1083545

Nielsdóttir, M. C., C. M. Moore, R. Sanders, D. J. Hinz, and E. P. Achterberg. 2009. Iron limitation of the postbloom phytoplankton communities in the Iceland Basin. Global Biogeochem. Cycles **23**: GB3001. doi:10.1029/2008GB003410

Panzeca, C., A. J. Beck, K. Leblanc, G. T. Taylor, D. A. Hutchins, and S. A. Sañudo-Wilhelmy. 2008. Potential cobalt limitation of vitamin B12 synthesis in the North Atlantic Ocean. Global Biogeochem. Cycles **22**: GB2029. doi:10.1029/2007GB003124

Parkhill, J., G. Maillet, and J. J. Cullen. 2001. Fluorescence-based maximal quantum yield for PSII as a diagnostic of nutrient stress. J. Phycol. **37**: 517–529. doi:10.1046/j.1529-8817.2001.037004517.x

Passow, U., and A. L. Alldredge. 1994. Distribution, size and bacterial colonization of transparent exopolymer particles (TEP) in the ocean. Mar. Ecol. Prog. Ser. **113**: 185–198. doi:10.3354/meps113185

Price, N. M., B. A. Ahner, and F. M. M. Morel. 1994. The equatorial Pacific Ocean: Grazer-controlled phytoplankton populations in an iron-limited ecosystem. Limnol. Oceanogr. **39**: 520–534. doi:10.4319/lo.1994.39.3.0520

Rapp, I., C. Schlosser, D. Rusiecka, M. Gledhill, and E. P. Achterberg. 2017. Automated preconcentration of Fe, Zn, Cu, Ni, Cd, Pb, Co, and Mn in seawater with analysis using high-resolution sector field inductively-coupled plasma mass spectrometry. Anal. Chim. Acta **976**: 1–13. doi:10.1016/j.aca.2017.05.008

Raven, J. A. 1987. The role of vacuoles. New Phytol. **106**: 357–422. doi:10.1111/j.1469-8137.1987.tb00122.x

Riebesell, U., D. A. Wolf-Gladrow, and V. Smetacek. 1993. Carbon dioxide limitation of marine phytoplankton growth rates. Nature **361**: 249–251. doi:10.1038/361249a0

Riebesell, U., and others. 2007. Enhanced biological carbon consumption in a high CO_2 ocean. Nature **450**: 545–549. doi:10.1038/nature06267

Riley, J. S., R. Sanders, C. Marsay, F. A. C. Le Moigne, E. P. Achterberg, and A. J. Poulton. 2012. The relative contribution of fast and slow sinking particles to ocean carbon export. Global Biogeochem. Cycles **26**: 1–10. doi:10.1029/2011GB004085

Ryan-Keogh, T. J., and others. 2013. Spatial and temporal development of phytoplankton iron stress in relation to bloom dynamics in the high-latitude North Atlantic Ocean. Limnol. Oceanogr. **58**: 533–545. doi:10.4319/lo.2013.58.2.0533

Rynearson, T. A., K. Richardson, R. S. Lampitt, M. E. Sieracki, A. J. Poulton, M. M. Lyngsgaard, and M. J. Perry. 2013. Major contribution of diatom resting spores to vertical flux in the sub-polar North Atlantic. Deep-Sea Res. Part I Oceanogr. Res. Pap. **82**: 60–71. doi:10.1016/j.dsr.2013.07.013

Saito, M. A., T. J. Goepfert, and J. T. Ritt. 2008. Some thoughts on the concept of colimitation: Three definitions and the importance of bioavailability. Limnol. Oceanogr. **53**: 276–290. doi:10.4319/lo.2008.53.1.0276

Sanders, R., and others. 2014. The biological carbon pump in the North Atlantic. Prog. Oceanogr. **129**: 200–218. doi:10.1016/j.pocean.2014.05.005

Sanders, R., and others. 2016. Controls over Ocean Mesopelagic Interior Carbon Storage (COMICS): Fieldwork, synthesis and modelling efforts. Front. Mar. Sci. **3**: 136. doi:10.3389/fmars.2016.00136

Schartau, M. A., and others. 2007. Modelling carbon overconsumption and the formation of extracellular particulate organic carbon. Biogeosciences **4**: 433–454. doi:10.5194/bg-4-433-2007

Schoffman, H. and N. Keren, 2019. Function of the IsiA pigment–protein complex in vivo. Photosynth. Res. **141**: 343–353. doi:10.1007/s11120-019-00638-5

Siegel, D.A., S.C. Doney, and J.A Yoder, 2002. The North Atlantic spring phytoplankton bloom and Sverdrup's critical depth hypothesis. Science, **296**: 730–733. doi:10.1126/science.1069174

Schrader, P. S., A. J. Milligan, and M. J. Behrenfeld. 2011. Surplus photosynthetic antennae complexes underlie diagnostics of iron limitation in a cyanobacterium. PLoS One **6**: e18753. doi:10.1371/journal.pone.0018753

Sedwick, P. N., P. W. Bernhardt, M. R. Mulholland, R. G. Najjar, L. M. Blumen, B. M. Sohst, C. Sookhdeo, and B. Widner. 2018. Assessing phytoplankton nutritional status and potential impact of wet deposition in seasonally oligotrophic waters of the Mid-Atlantic Bight. Geophys. Res. Lett. **45**: 3203–3211. doi:10.1002/2017GL075361

Seymour, J. R., S. A. Amin, J. B. Raina, and R. Stocker. 2017. Zooming in on the phycosphere: The ecological interface for phytoplankton–bacteria relationships. Nat. Microbiol. **2**: 17065. doi:10.1038/nmicrobiol.2017.65

Siegel, D. A., and others. 2016. Prediction of the export and fate of global ocean net primary production: The EXPORTS Science Plan. Front. Mar. Sci. **3**. doi:10.3389/fmars.2016.00022

Sieracki, M. E., P. G. Verity, and D. K. Stoecker. 1993. Plankton community response to sequential silicate and nitrate depletion during the 1989 North Atlantic spring bloom. Deep-Sea Res. Part II Top. Stud. Oceanogr. **40**: 213–225. doi:10.1016/0967-0645(93)90014-E

Smetacek, V. 1999. Diatoms and the ocean carbon cycle. Protist **150**: 25–32. doi:10.1016/S1434-4610(99)70006-4

Smetacek, V. 2018. Seeing is believing: Diatoms and the ocean carbon cycle revisited. Protist **169**: 791–802. doi:10.1016/j.protis.2018.08.004

Smetacek, V. S. 1985. Role of sinking in diatom life-history cycles: Ecological, evolutionary and geological significance. Mar. Biol. **84**: 239–251. doi:10.1007/BF00392493

Smith, K.L., H. A. Ruhl, C. L. Huffard, Messié, M. and Kahru, 2018. Episodic organic carbon fluxes from surface ocean to abyssal depths during long-term monitoring in NE Pacific. Proc. Natl. Acad. Sci. **115**: 12235–12240. doi:10.1073/pnas.1814559115

Sverdrup, H. U. 1953. On vernal blooming of phytoplankton. J. Conseil. Int. Exp. Mer. **18**: 287–295. doi:10.1093/icesjms/18.3.287

Takeda, S. 1998. Influence of iron availability on nutrient consumption ratio of diatoms in oceanic waters. Nature **393**: 774–777. doi:10.1038/31674

Taucher, J., K. G. Schulz, T. Dittmar, U. Sommer, A. Oschlies, and U. Riebesell. 2012. Enhanced carbon overconsumption in response to increasing temperatures during a mesocosm experiment. Biogeosciences **9**: 3531–3545. doi:10.5194/bg-9-3531-2012

Toggweiler, J. R. 1993. Carbon overconsumption. Nature **363**: 210–211. doi:10.1038/363210a0

Trees, C. C., D. K. Clark, R. R. Bidigare, M. E. Ondrusek, and J. L. Mueller. 2000. Accessory pigments versus chlorophyll a concentrations within the euphotic zone: A ubiquitous relationship. Limnol. Oceanogr. **45**: 1130–1143. doi:10.4319/lo.2000.45.5.1130

Turner, J. T. 2002. Zooplankton fecal pellets, marine snow and sinking phytoplankton blooms. Aquat. Microb. Ecol. **27**: 57–102. doi:10.3354/ame027057

Uitz, J., H. Claustre, A. Morel, and S. B. Hooker. 2006. Vertical distribution of phytoplankton communities in open ocean: An assessment based on surface chlorophyll. J. Geophys. Res. Oceans **111**: C08005. doi:10.1029/2005JC003207

Van Heukelem, L., and C. S. Thomas. 2001. Computer-assisted high-performance liquid chromatography method development with applications to the isolation and analysis of phytoplankton pigments. J. Chromatogr. A **910**: 31–49. doi:10.1016/S0378-4347(00)00603-4

Verdugo, P., A. L. Alldredge, F. Azam, D. L. Kirchman, U. Passow, and P. H. Santschi. 2004. The oceanic gel phase: A bridge in the DOM–POM continuum. Mar. Chem. **92**: 67–85. doi:10.1016/j.marchem.2004.06.017

Verity, P. G., D. K. Stoecker, M. E. Sieracki, and J. R. Nelson. 1993. Grazing, growth and mortality of microzooplankton during the 1989 North Atlantic spring bloom at 47 N, 18 W. Deep-Sea Res. Part I Oceanogr. Res. Pap. **40**: 1793–1814. doi:10.1016/0967-0637(93)90033-Y

Welschmeyer, N. A. 1994. Fluorometric analysis of chlorophyll a in the presence of chlorophyll b and pheopigments. Limnol. Oceanogr. **39**: 1985–1992. doi:10.4319/lo.1994.39.8.1985

Wetz, M. S., and P. A. Wheeler. 2003. Production and partitioning of organic matter during simulated phytoplankton blooms. Limnol. Oceanogr. **48**: 1808–1817. doi:10.4319/lo.2003.48.5.1808

Williams, R., and H. Claustre. 1991. Photosynthetic pigments as biomarkers of phytoplankton populations and processes involved in the transformation of particulate organic matter at the Biotrans site (47°N, 20°W). Deep-Sea Res. A **38**: 347–355. doi:10.1016/0198-0149(91)90072-N

Acknowledgments

We thank the captain, crew, technicians, and scientists onboard the *RRS Discovery* cruise DY080. A. Mutzberg, K. Nachtigall, and T. Klüver are thanked for technical laboratory assistance. M. Gledhill is thanked for instruction on the POC/N analyses and A. Stuhr for assistance with the microscopy analyses. M. Moore, A. Annett, M. Humphreys, K. Hendry, and C. Burd are thanked for helping with cruise logistics. Three anonymous reviewers are thanked for their constructive comments that improved the manuscript. This work was partly funded by a Marie Skłodowska-Curie Postdoctoral European Fellowship awarded to T.J.B. (OceanLiNES; project ID 658035). Funding from the Kuwait Institute for Scientific Research for the doctoral studies of A.A.A. is acknowledged. The cruise was funded by the Natural Environment Research Council (NERC; grant NE/M017990/1).

Conflict of Interest

None declared.

Submitted 20 June 2019
Revised 23 August 2019
Accepted 30 September 2019

Associate editor: Ilana Berman-Frank